FEM Simulation Comparisons of Backward Extrusion

G.Y. Tzou, C.C. Hsu, C.T. Kuo

Department of Mechanical and Automation Engineering, Kao Yuan University, Luzhu, Kaohsiung, 821, Taiwan

E-mail:gowyitzou@cc.kyu.edu.tw

Abstract - This study with constant shear friction uses DEFORM 2D software to perform FEM simulation of backward extrusion, and compares to SUPERFORM FEM simulation to realize the variations of forming conditions with the punch force and the final cup height. Effects of frictional factor, punch nose face angle, punch nose radius, and punch seizing length on equivalent stress, equivalent strain, velocity field, punch force, and deformed shape can be explored. Meanwhile using both FEM softwares to simulate can realize variations of both models in order to provide the reference of backward extrusion.

Keywords- Constant shear friction, Backward extrusion, Punch force, Final cup height, Equivalent stress, Equivalent strain.

I. INTRODUCTION

Chen et al.[1] studies effects of the extrusion ratio of backward extrusion on grain refinement of AZ31 magnesium alloy. The result points out that as heating the material to 250°C the better the mechanical property the larger the extrusion ratio. Matsumoto et al. [2] explores the forming limit of AZ31B magnesium alloy using cold backward extrusion and cylinder compression. The punch adopts the cone taper to realize the effect of cone taper on the strain. As the cone taper increases, the strain induced increases. Long et al.[3] use ABAQUS commercial analysis software to analyze the plastic deformation, temperature distribution, and elastic deformation of dies. Bakhshi-Jooybari and Saboori [4,5] think how to increase the dies life and avoid the dies failure are very important in the metal forming process. Different mold shapes, cones and arcs have been considered to perform the forward and backward extrusions, besides the slab method and ABAQUS software analysis have been used to get the optimal forming force. Uyyuru et al. [6] uses new physical model and Deform FEM simulation to explore the plastic deformation and final cup height of Al alloy under different frictions in backward extrusion. Kim et al. [7] performs the backward extrusion of square shape under large aspect ratio, as the aspect ratio is larger, the final cup height is hard to control; where the earring is occurred. In the paper MSC Superforge software is used to do simulation analysis, and use the ring test to obtain the frictional factor and frictional coefficient with AL1100-0 work-piece. Barisic et al. [8] use Lab View commercial software to design multi-factors mathematical modal according to the compression experiment to get the forming force of backward extrusion by the regression analysis. Li et al. [9] explore backward extrusion of the composite material with AL6061 alloy and silicon to observe the grain size and distribution under various extrusion ratios using SEM. Danckert [10] studies the influence of the punch land in backward can extrusion. Adjusting the punch inclined to reduce the vibration of punch force and non-uniform cup thickness using the FEM analysis. Hur et al. [11] investigate into the elastic behaviour for stress ring of dies using ANSYS, and using DEFORM to get the backward extrusion forming process.

In the study, the Deform and Superform softwares have been used to explore the variations and acceptance. Effects of frictional factor, punch nose face angle, punch nose radius, and punch seizing length on effective equivalent stress, equivalent strain, velocity field, punch force, and deformed shape can be explored.

II. FEM SIMULATIONS

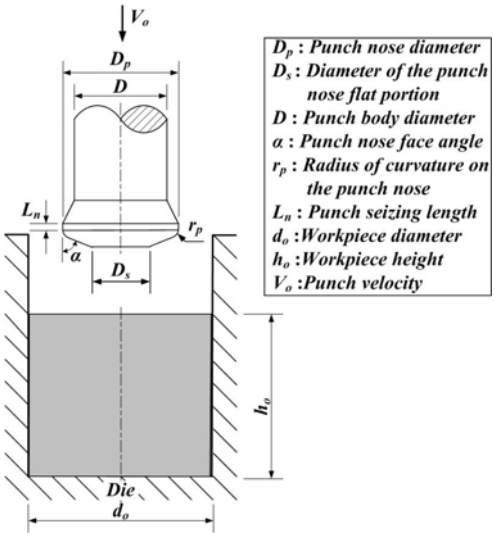

Fig. 1 Schematic diagram of backward extrusion.

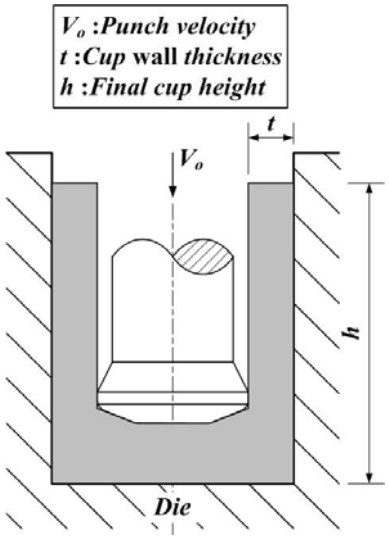

Fig. 2 Schematic diagram after backward extrusion.

The schematic diagram of backward extrusion is shown in Fig. 1. In the Fig. 1, the work-piece is a cylinder , the punch is going down with the velocity, V_0 , the friction is assumed as a constant shear friction.

The schematic diagram after the backward extrusion is shown in Fig. 2, the final cup height can be obtained. The work-piece material is a copper, C1100, the flow stress is shown in Fig. 3. As seen in Fig. 3, the solid line is obtained by the experiment; the dash line is obtained by the curve fitting with power law, $\sigma = 417.69\varepsilon^{0.046}$.

Firstly, the preprocess set up by CAD considering axis-symmetry is shown in Fig. 4. With a view to avoiding the calculation error, the convergence analysis is necessary to perform as shown in Fig. 5. From Fig. 5, the element is a quadrilateral with four nodes, and the 8 various element numbers are considered from rough to fine mesh. The friction is 0.1; the punch nose face angle is 80 °; the punch velocity is 1mm/s. The convergence error is ±1% in this analysis; the formula is expressed as below:

$$\text{Convergence error}(\%) = \frac{Result_n - Result_{n-1}}{Result_n} \times 100\% \qquad (1)$$

The exact datum are shown in Table I; the model 5 (element numbers 7000) is good for the analysis, the convergence error is -0.19%.

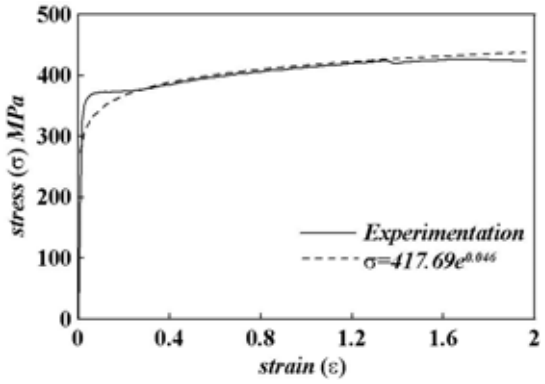

Fig. 3 Flow stress of work-piece material.

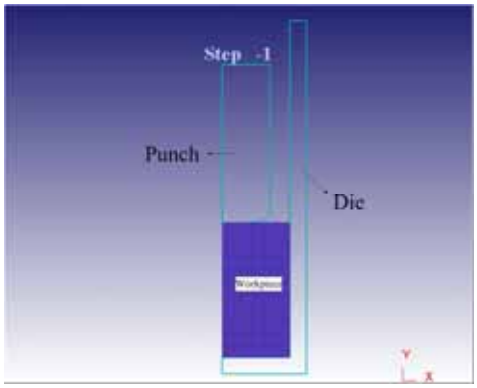

Fig. 4 FEM simulation preprocess setup by CAD.

TABLE I
THE DATUM FOR CONVERGENCE ANALYSIS

Model	Total No. of Element	Punch Force(kN)	Convergence Error(%)
1	5000	758.2	
2	5460	754.4	-0.50889
3	6050	751.4	-0.40325
4	6498	753.1	0.230347
5	**6962**	**751.6**	**-0.19688**
6	7442	753.4	0.241897
7	7928	757.2	0.491692
8	8450	755.6	-0.20174

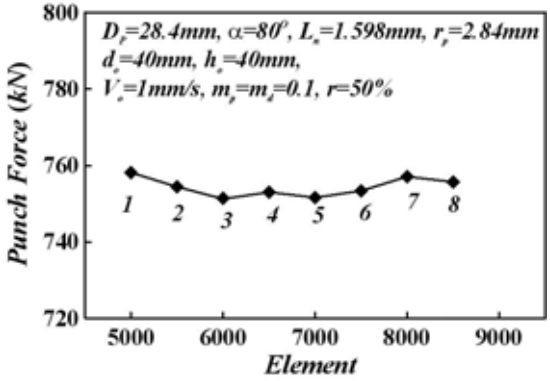

Fig. 5 Convergence analysis for 8 models.

III. RESULTS AND DISCUSSIONS

In this paper, the variations of results obtained by Deform and Superform softwares have been compared. The simulation conditions are demonstrated in Table II.

TABLE II
SIMULATION CONDITIONS FOR BACKWARD EXTRUSION

Workpiece size (*mm*)	h_o: *40*, d_o: *20*
Punch velocity (*mm/sec*), V_o	*1*
radius of curvature (*mm*), r_p	*1.42, 2.13, 2.84*
Punch seizing length (*mm*), L_n	*1.589, 2.664,3.73*
Punch nose face angle, α	*80°, 83°, 85°*
Frictional factor, *m*	*0.05, 0.1, 0.15, 0.2*

Fig. 6 shows variations of punch force with frictional factor for both FEM simulations. The punch force increases with an increase of frictional factor for both FEM simulations. The punch force obtained from Deform is slightly higher than that obtained from Superform. The error is round 3% between both FEM simulations.

Fig. 7 shows variations of final cup height with frictional factor for both FEM simulations. The final cup height obtained from Deform is slightly lower than that obtained from Superform. The final cup height slightly decreases with an increase of frictional factor for both FEM simulations. The error is round 1.5% between both FEM simulations. As

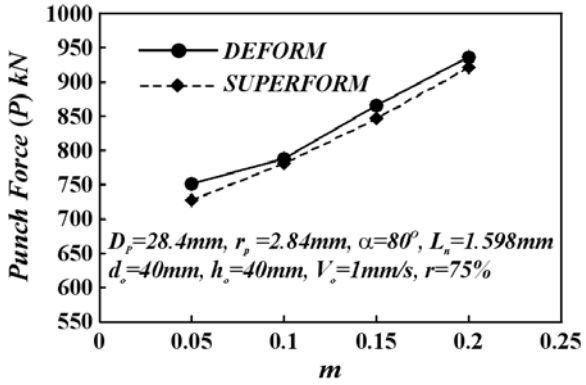

Fig. 6 Variations of punch force with frictional factor for both FEM simulations.

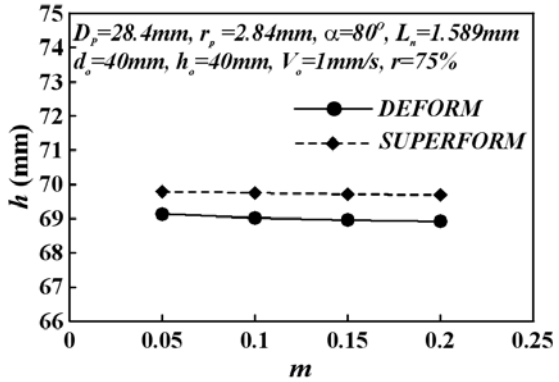

Fig. 7 Variations of final cup height with frictional factor for both FEM simulations.

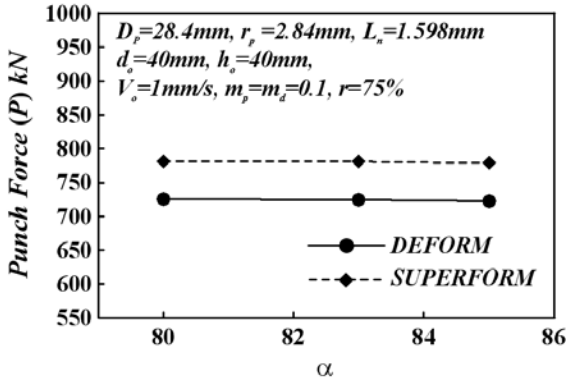

Fig. 8 Variations of punch force with punch nose face angle for both FEM simulations.

the frictional factor increases the flow resistance increases, therefore the final cup height is reduced.

Fig. 8 show variations of punch force with punch nose face angle for both FEM simulations. The punch force slightly decreases with an increase of punch nose face angle for both FEM simulations. That is because the contact area is reduced as the punch nose face angle increases. The punch force obtained from Deform is slightly lower than that obtained from Superform. The error is round 8% between both FEM simulations.

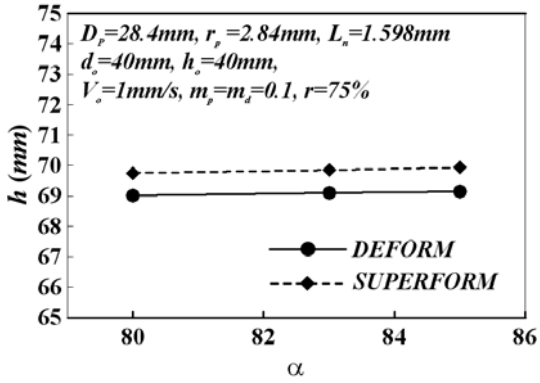

Fig. 9 Variations of final cup height with punch nose face angle for both FEM simulations.

Fig. 9 shows variations of final cup height with punch nose face angle for both FEM simulations. The final cup height obtained from Deform is slightly lower than that obtained from Superform. The final cup height slightly increases with an increase of punch nose face angle for both FEM simulations. That is because the contact area is reduced so that the material is easy to flow as the punch nose face angle increases. The error is round 1.5% between both FEM simulations. As the punch nose face angle increases the flow resistance decreases, therefore the final cup height is increased.

Fig. 10 show variations of punch force with punch nose radius for both FEM simulations. The punch force slightly decreases with an increase of punch nose radius for both FEM simulations. That is because the material flow smoothly as the punch nose radius increases. The punch force obtained from Deform is slightly lower than that obtained from Superform. The error is round 8% between both FEM simulations.

Fig. 11 shows variations of final cup height with punch nose radius for both FEM simulations. The final cup height obtained from Deform is slightly lower than that obtained from Superform. The final cup height slightly increases with an increase of punch nose radius for both FEM simulations. That is because the contact length is more so that the material flow rate is slow as the punch nose radius increases. The error is round 1.5% between both FEM simulations.

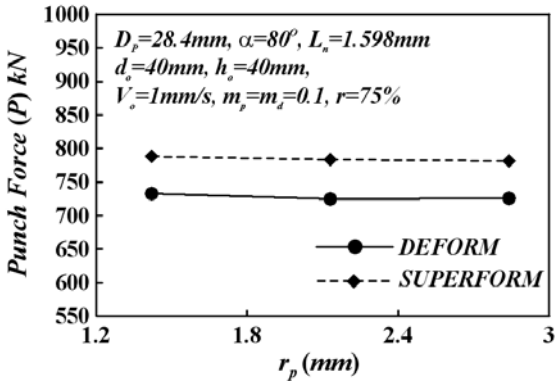

Fig. 10 Variations of punch force with punch nose radius for both FEM simulations.

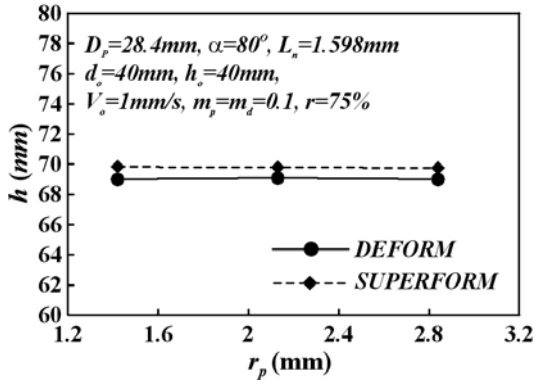

Fig. 11 Variations of final cup height with punch nose radius for both FEM simulations.

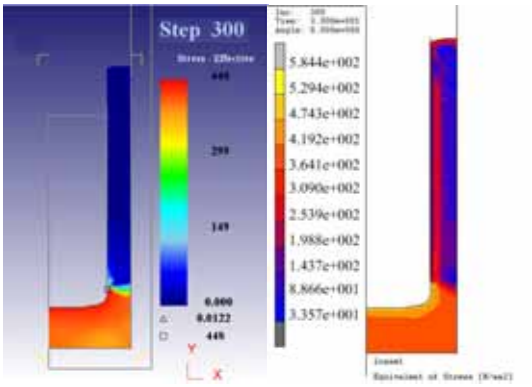

DEFORM SUPERFORM

Fig. 12 Equivalent stresses for both FEM simulations. (D_P=28.4mm, r_p=2.84mm,L_n=1.598mm,α=80°,d_o=40mm,h_o=40mm,V_o=1mm/s, m_p=m_d=0.1)

Fig. 12 shows equi valent stresses for both FEM simulations. The maximum equivalent stress occurs near the seizing part for both simulations. The maximum equivalent stress from Deform (448MPa) is smaller than that from Superform (584MPa).

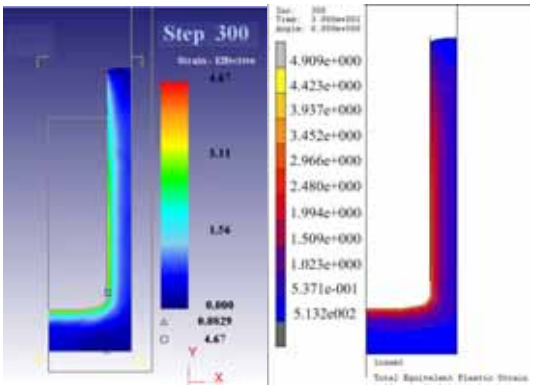

DEFORM SUPERFORM

Fig. 13 Equivalent strains for both FEM simulations. (D_P=28.4mm, r_p=2.84mm,L_n=1.598mm,α=80°,d_o=40mm,h_o=40mm,V_o=1mm/s, m_p=m_d=0.1)

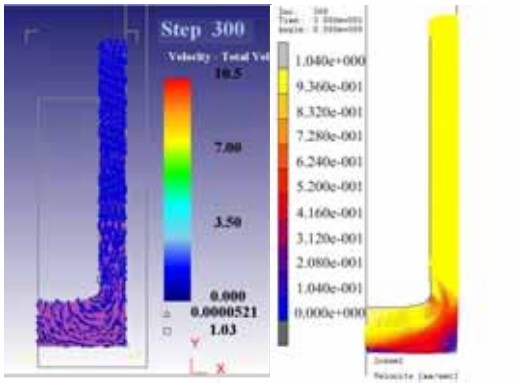

DEFORM SUPERFORM

Fig. 14 Velocity field for both FEM simulations. (D_P=28.4mm, r_p=2.84mm,L_n=1.598mm,α=80°,d_o=40mm,h_o=40mm,V_o=1mm/s, m_p=m_d=0.1)

Fig. 13 shows equi valent strains for bot h FEM simulations. The maximum equivalent strain occurs near the exit of sei zing part for bot h simulations. The maximum equivalent strain from Deform (4.67mm/mm) is smaller than that from Superform (4.9 mm/mm).

Fig. 14 shows vel ocity field for both FEM simulations. The maximum velocity occurs near the exit of seizing part for both simulations. The m aximum velocity from Deform (1.03 mm/s) is slig htly smaller than that from Superform (1.04 mm/s). It is noted the dead zone occurs in the bottom die angle.

III. CONCLUSIONS

Through a seri es of si mulation results of backward extrusion, the effects of form ing conditions on the punch force and fi nal cup hei ght have been summarized in Table III.

TABLE III
SIMULATION RESULTS FOR BACKWARD EXTRUSION

	Puuch Force		Final Cup Height	
	DEFORM	SUPER FORM	DEFORM	SUPER FORM
m_d, m_p	↗	↗	↘	↘
α	↘	↘	↗	↗
r_p	↘	↘	↗	↗
L_n	↗	↗	↘	↘

In Table III, " ↗"denotes the result increases with an increase of forming condition; " ↘ "denotes the result decreases with an increase of forming condition. The major results are described as below:

1) The punch force i ncreases with increasing frictional factor and seizing length, whereas decreases with increasing punch nose face angle and punch nose radius.

2) The final cup height decreases with increasing frictional factor and seizing length, whereas increases with increasing punch nose face angle and punch nose radius.

3) The results from both simulations reveal allowable errors and show the same trend.

ACKNOWLEDGMENT

Thanks for financial support from National Science Council(Grants: NSC 99-2221-E-244-005).

REFERENCES

[1] Y. Chen, Q. Wang, J. Peng, C. Zhai, W. Ding, Effects of Extrusion Ratio on the Microstructure and Mechanical Properties of AZ31 Mg Alloy, *Journal of Materials Processing Technology*, Volume: 182, Issue: 1-3, February 2, 2007, pp. 281-285

[2] R. Matsumoto, T. Kubo, K. Osakada, Fracture of Magnesium Alloy in Cold Forging, *CIRP Annals - Manufacturing Technology*, Volume: 56, Issue: 1, 2007, pp. 293-296

[3] H. Long, Quantitative Evaluation of Dimensional Errors of Formed Components in cold Backward cup Extrusion, *Journal of Materials Processing Technology*, Volume: 177, Issue: 1-3, July 3, 2006, pp. 591-595

[4] M. Bakhshi-Jooybari, M. Saboori, S.J. Hosseinipour, et al. , Experimental and Numerical Study of Optimum die Profile in Backward rod Extrusion, *Journal of Materials Processing Technology*, Volume: 177, Issue: 1-3, July 3, 2006, pp. 596-599

[5] M. Saboori, M. Bakhshi-Jooybari, M. Noorani-Azad, A. Gorji, Experimental and Numerical Study of Energy Consumption in Forward and Backward rod Extrusion, Journal of Materials Processing Technology, Volume: 177, Issue: 1-3, July 3, 2006, pp. 612-616

[6] R.K. Uyyuru, H. Valberg, Physical and Numerical Analysis of the Metal Flow Over the Punch Head in Backward cup Extrusion of Aluminum, *Journal of Materials Processing Technology*, Volume: 172, Issue: 2, February 28, 2006, pp. 312-318

[7] S.H. Kim, S.W. Chung, S. Padmanaban, Investigation of Lubrication Effect on the Backward Extrusion of Thin-Walled Rectangular Aluminum case with Large Aspect Ratio, *Journal of Materials Processing Technology*, Volume: 180, Issue: 1-3, December 1, 2006, pp. 185-192

[8] B. Barisic, G. Cukor, M. Math, Estimate of Consumed Energy at Backward Extrusion Process by Means of Modelling Approach, *Journal of Materials Processing Technology*, Volume: 153-154, November 10, 2004, pp. 907-912

[9] J.H. Li, C.F. Li, The effect of Backward Extrusion on the Whisker Morphology of SiC_w/6061Al, *Journal of Materials Processing Technology*, Volume: 151, Issue: 1-3, September 1, 2004, pp. 302-306

[10] J. Danckert, The Influence of the Punch Land in Backward can Extrusion, *CIRP Annals - Manufacturing Technology*, Volume: 53, Issue: 1, 2004, pp. 227-230

[11] K.D. Hur, Y. Choi, H.T. Yeo, A Design Method for Cold Backward Extrusion using FE Analysis, *Finite Elements in Analysis and Design*, Volume: 40, Issue: 2, December, 2003, pp. 173-185